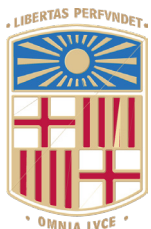


Book of Tutorials and Abstracts



European Microbeam Analysis Society

EMAS 2025

18th
EUROPEAN WORKSHOP

on

MODERN DEVELOPMENTS AND APPLICATIONS IN MICROBEAM ANALYSIS

11 to 15 May 2025
at the
TecnoCampus
Mataró (Barcelona), Spain

Organized in collaboration with the
Universitat de Barcelona, Spain

EMAS

European Microbeam Analysis Society eV

www.microbeamanalysis.eu/

This volume is published by:

European Microbeam Analysis Society eV (EMAS)

EMAS Secretariat

c/o Eidgenössische Technische Hochschule, Institut für Geochemie und Petrologie

Clausiusstrasse 25

8092 Zürich

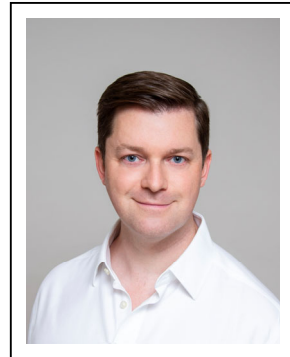
Switzerland

© 2025 *EMAS* and authors

ISBN 978 90 8227 6985

NUR code: 972 – Materials Science

All rights reserved. No part of this publication may be reproduced, stored in a retrieval system, or transmitted in any form or by any means, electronic, mechanical, by photocopying, recording or otherwise, without the prior written permission of *EMAS* and the authors of the individual contributions.



CORRELATED MECHANICAL MICROSCOPY USING NANOINDENTATION, EDS, AND EBSD MAPPING ON A SEYMCHAN METEORITE FRAGMENT

Jeffrey M. Wheeler¹, S.-H. Lee² and S. Korte-Kerzel²

1 Oxford Instruments - FemtoTools AG
Furtbachstrasse 4, CH-8107 Buchs, Switzerland
2 RWTH Aachen University, Institut für Metallkunde und Materialphysik
52074 Aachen, Germany
e-mail: jeff.wheeler@oxinst.com

Jeffrey M. Wheeler is a leader in the fields of nanoindentation and micromechanics, particularly at high temperatures, with over 100 scientific publications over the last two decades. He received his PhD in Materials Science and Metallurgy from the University of Cambridge in 2009. His research focusses on using correlated analytical and nanomechanical techniques to understand deformation mechanisms in a wide range of materials. He is currently a scientific advisor at Oxford Instruments.

1. ABSTRACT

In the 30 years since the initial development of nanoindentation, the technique has been extensively applied to measure a large number of different types of mechanical properties. Chief among these is hardness and elastic modulus, but other properties such as fracture toughness, strain rate sensitivity, adhesion, nucleation stress have also been investigated using nanoindentation. In the last decade, a major effort has been made by manufacturers to improve the speed of nanoindentation testing. This has transformed the technique from being primarily useful for local investigations with limited statistics into a 2D mechanical microscopy technique with sub-micron resolution [1]. Today, statistical mechanical property distributions at this scale can be obtained that represent the local mechanical performance of microstructural features (phases, interfaces, grains orientations, etc.). As a result, a wide range of new opportunities for mechanical microstructural investigations now exist with each type of mechanical property which has been previously investigated using nanoindentation now also available as an imaging modality for mechanical microscopy.

However, the true power of this technique is unlocked when it is applied correlatively with microbeam analysis techniques to directly elucidate mechanical properties-composition-structure relationships. To connect the mechanical performance of each feature to its structural and/or compositional data, additional data from microbeam analysis techniques – such as energy-dispersive X-ray spectrometry (EDS) or electron back-scattered diffraction (EBSD) – is required over the same microstructural region. When these two datasets are properly aligned to the same coordinate axes and registered, it allows correlative mechanical microscopy. This provides structural, compositional, and mechanical information on each local sample volume within the mapped region. Relationships between crystallographic phases and orientations, composition, and mechanical properties can, therefore, be easily determined for every feature within the microstructure. In previous work, we have demonstrated correlated mechanical microscopy with both EDS and EBSD separately and concurrently [2]. The combination of these techniques provides incredible insight into the relationships between mechanical properties, composition, and crystallographic phase and orientation. Their mutual micrometric length scale allows them to locally interrogate with high spatial resolution. However, correlation with each of these techniques presents distinct challenges.

Correlated mechanical microscopy with EDX can be performed in a relatively straightforward manner by simply performing a nanoindentation map and then performing an EDS map on the same region with matching resolution. As the nanoindentation deformation does not change the local composition, the EDS mapping can easily be done after the indentation map using the indentation grid as a fiducial for alignment. This provides an ideal 1:1 correlation between the two datasets, as previously demonstrated in a combinatorial investigation of the Ni-Ta system [3].

Correlating mechanical microscopy with EBSD is more challenging due to two factors. Alignment is more challenging due to the 70° tilted orientation of the sample required in the scanning electron microscope (SEM) for EBSD acquisition. Further, EBSD should ideally be performed before the nanoindentation map, as the indentation process produces surface deformation which might affect the EBSD pattern quality. Therefore, additional fiducial markings are required to facilitate alignment of the two grids. However, some distortion of the data matrices is likely to occur due to the angular tilt mentioned above, requiring an affine transformation and interpolation of the datasets to achieve correlation [4].

In this work, nanoindentation, EDS and EBSD mapping are used to perform correlative mechanical microscopy on a fragment of the Seymchan meteorite. Meteorites often feature complex microstructures featuring compositional gradients and multiple phases. Correlative techniques are very important for data analysis to identify trends between the compositional and mechanical techniques, as analysis of one technique alone may be insufficient for data segmentation or deconvolution of overlapping clusters [5]. Details of the approach are described, particularly the system concerns, and the ability of the correlative approach to identify individual orientations and phases is demonstrated and discussed.

2. MATERIALS AND METHODS

The Seymchan meteorite (approx. Fe-9Ni-0.5Co) sample was extracted with a size of about 1×1×0.5 cm³, respectively, by electrical discharge machining or with a diamond wire saw. A metallographic preparation was then carried out to ensure an appropriately flat and deformation-free surface suitable for both, combined EDS-EBSD and nano-indentation experiments. Initially, the samples were mechanically ground and then polished using water-based diamond suspensions of progressively increasing fineness to a final 1 μm particle size. In order to minimise the surface relief while maintaining a strain-free surface for good Kikuchi patterns a short final mechanical polishing was performed with 0.25 μm colloidal silica (OP-S, Struers, Denmark) on a neoprene polishing cloth (OP-Chem, Struers).

Nanoindentation mapping was performed using a FT-I04 Femto-Indenter (FemtoTools AG, Switzerland) equipped with an FT-S20,000 sensor and a diamond Berkovich tip. Each indentation was performed using continuous stiffness measurement (CSM) method [6] in displacement control. An oscillation frequency of 150 Hz and a proportionally scaled amplitude that linearly increased from 0.5 to 2.5 nm with increasing depth was used. A map of 200×150 indentations was performed with a maximum depth of 190 nm and a 2 μm spacing. This ensured an indentation depth/spacing ratio of 10 was maintained [7]. Representative values for each indentation were determined from the mean of values measured at contact depths above 50 % of the target depth for elastic modulus and 80 % for hardness to minimize errors from indentation size effects.

Microstructural analyses were performed using analytical SEM, backscattered electron (BSE) imaging, and combined EDS-EBSD in a Hitachi SU-5000 (Oxford Instruments UltimMax 100 EDS and Symmetry 2 EBSD detector) at 20 kV. They were recorded with a 1 μm step size across the indented area for the Seymchan meteorite and were analysed using the free MTEX 5.7.0 toolbox based on MATLAB® [8].

To correlate and register the nanoindentation, EDS, and EBSD measurements, a dedicated Python library ‘PYXC’ was employed, as described in more detail in Seehaus *et al.* [2]. The library corrects systematic distortions that occur with various measurement methods, aligns the data layers to a reference image and queries the data by an arbitrary X or Y coordinate. This open-source library is now available online: <https://zenodo.org/record/8322342>.

Due to the flexibility of the library, almost any 2-dimensionally sampled data with or without X or Y coordinates can be correlated. However, to achieve the correlation without coordinate information (e.g., an image from an optical microscope or a scanning electron microscope) an assignment of missing X or Y coordinates based on respective pixel indices is required. Any data with X or Y coordinates can directly be loaded into the library. Full details on the developed correlation procedure and methods for extraction of elastic tensors from correlated data are presented in reference [2].

3. RESULTS AND DISCUSSION

The Seymchan meteorite sample was used in order to demonstrate the combined capabilities of correlated mechanical microscopy. A region of Widmanstätten bands, also known as Thomson structures, was selected for investigation, as it is comprised of several long grains of body-centred-cubic kamacite (referred to hereafter as α) and thin seams of taenite/tetrataenite (referred to hereafter as γ) around the α -grains (Fig. 1). In addition, some hard, phosphorus-rich precipitates of schreibersite and fine-grained intermediate domains of α and γ are visible.

Figure 2 shows the results of the correlated mechanical microscopy study with aligned nanoindentation property, EDS, and EBSD maps. Several general trends between the phases are clear on first examination. The thin γ -regions between the larger α grains in the Widmanstätten bands display simultaneously the highest hardness and lowest reduced modulus values. These regions correspond to the highest nickel concentrations are often not well indexed by EBSD to a particular orientation, possibly due to a fine grain size, but largely share a common orientation. In general, a strong visual correlation can be noted between the regions with lower reduced modulus and the regions with high Ni-concentrations.

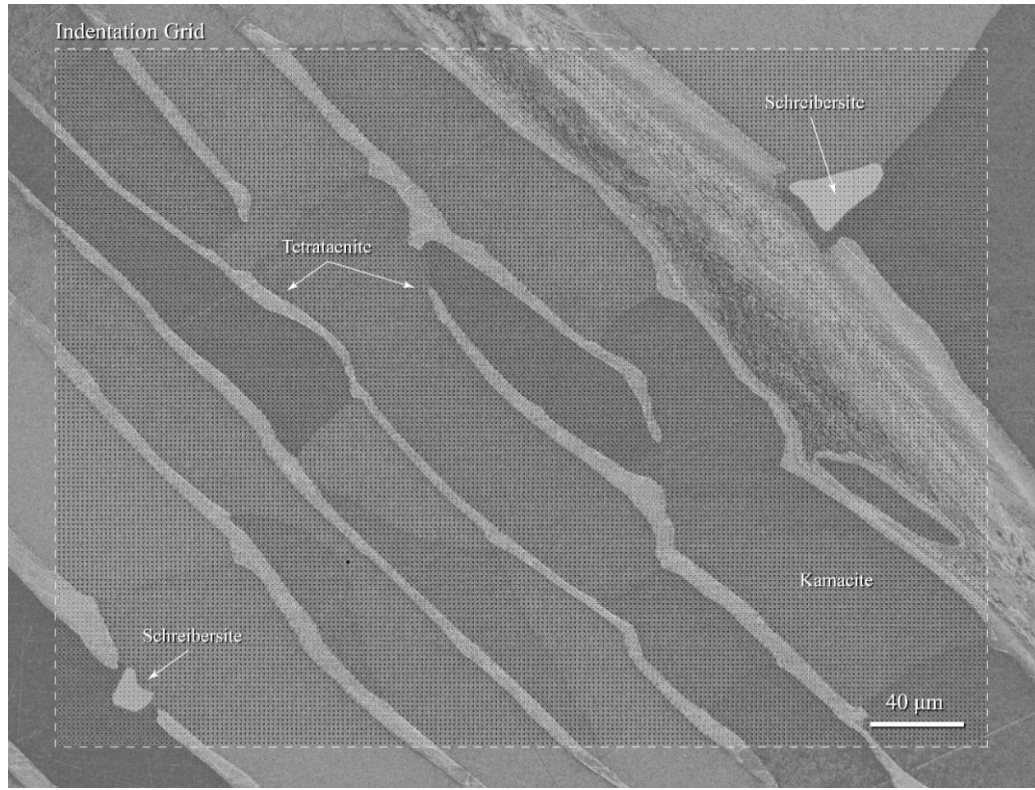


Figure 1. Backscattered electron micrograph of the investigated Widmanstätten region of the Seymchan meteorite showing the indentation grid with various regions and phases labelled.

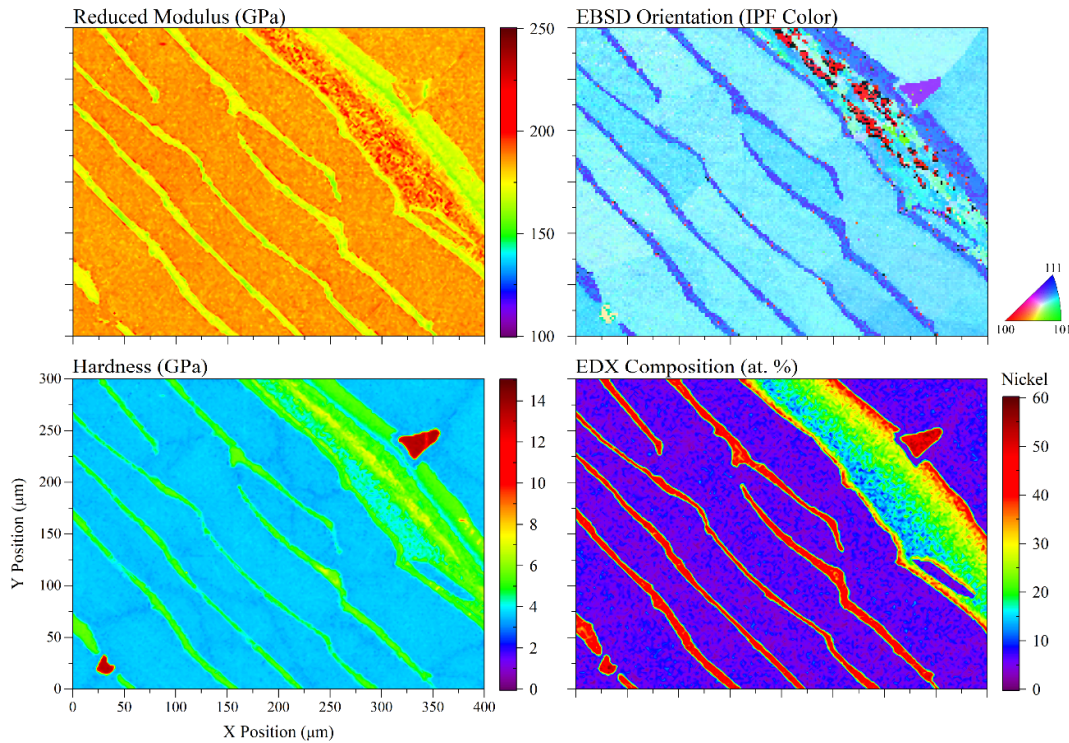


Figure 2. Mechanical microscopy results from the Seymchan meteorite with correlated indentation property maps with EBSD orientation and EDS Ni-concentration.

The kamacite, α -phase bands show a similar range of orientations, sky blue in the EBSD map with inverse pole figure (IPF) colouring, relatively near to the [111] direction. These α -grains all show relatively consistent indentation properties throughout without much internal scatter in hardness or reduced modulus. Some sub-grain boundaries can be seen within these bands in the back-scattered electron micrograph (Fig. 1) and in the EBSD orientation maps (Fig. 2).

Another small precipitate phase notable in the indentation property maps is a very high hardness schreibersite, $(\text{Fe},\text{Ni})_3\text{P}$ phase near the centre of the hardness map. As noted in another work [9], schreibersite displays very similar modulus to α -kamacite despite its high hardness. This was identified in EDS maps of P-concentration, but these are not shown here.

The compositional gradient at the border of the large kamacite grain at the far right of the region warrants some additional discussion. This feature forms as Ni is rejected from the α -phase grain, generating a high-Ni concentration at the border, which decreases with distance. This is very similar to compositional gradients observed at the borders of large α -phase, kamacite, bands in a Taza meteorite fragment previously [9]. At near equiatomic Fe- and Ni-concentrations, the tetrataenite, FeNi , phase forms which has high hardness and lower modulus compared to kamacite. This forms a distinct band within the gradient. Then as the Ni-concentration decreases, a nanocomposite “cloudy zone” region of very high hardness forms, which consists of tetrataenite in a taenite matrix, which is difficult for EBSD to index.

3.1. Correlated property distributions

Visual correlation of the salient features in the different characterisation modalities (nanoindentation, EDS, and EBSD) can provide insights into specific microstructural features. However, to extract statistical trends from these maps, it is useful to look at them in property space (Fig. 3), which provides a visual representation of major statistical clusters in terms of hardness and reduced modulus. In these plots, we can clearly identify three major clusters. The hardest of these is attributed to the schreibersite, phosphide phase, while the two lower clusters are attributed to tetrataenite (lower modulus/higher hardness) and kamacite (higher modulus/lower hardness).

To confirm the nature of these clusters, it is helpful to use correlated results from EDS and EBSD, provided by the colour coding of the plots in Fig. 3. This allows the compositional and orientation trends within the data to be visualised. By examining these plots, several features become clear. The second hardest cluster is confirmed as the tetrataenite γ -phase with orientations near [111] and the highest Ni concentrations (~ 50 at% Ni). This cluster contains a tight distribution in terms of mechanical properties, composition, and orientation. The highest modulus cluster, attributed to α -phase, is confirmed to be kamacite by its BCC crystal structure and low Ni-concentration (< 10 at%). This distribution has a relatively wide variation in reduced modulus, despite its largely consistent crystallographic orientation.

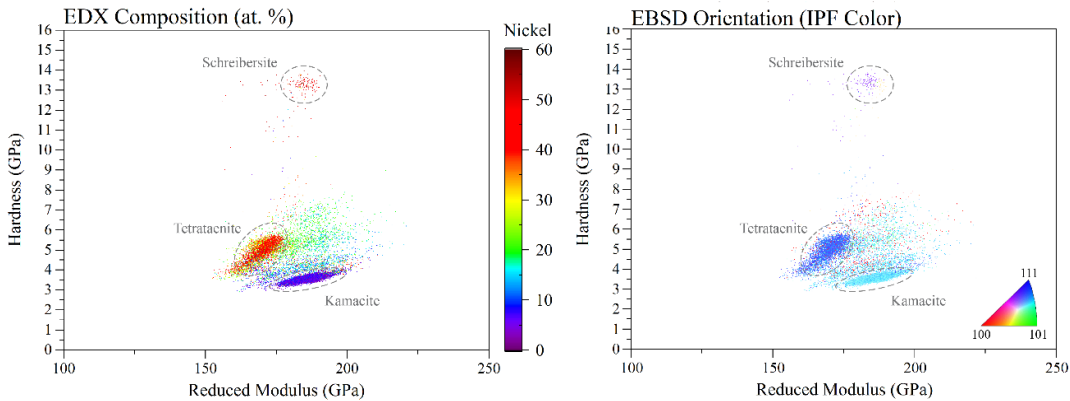


Figure 3. Correlated mechanical property distributions: 2D scatter plots with datapoints colour coded using correlated EDS and EBSD data.

There are a large number of intermediate value points between the tetrataenite and kamacite clusters. These are attributed to the compositional gradient or “cloudy zone” region, which is a fine nanocomposite admixture of the two phases over a range of Ni-concentrations, and this also contains the majority of points which were not indexed (black) by EBSD. This makes sense as the “cloudy zone” region contains the finest scale features in the map, which likely contain multiple phases under indentations of this size, preventing easy indexing.

3.2. Correlation challenges

While this investigation in correlated mechanical microscopy was successful in identifying the major phases within this region of the Seymchan meteorite fragment, it also reveals some challenges that the correlated approach highlights. In general, correlation can be challenging if there is insufficient statistical data or if there are features within the dataset that reduce alignment precision, such as noise within the data, complex grain boundary regions, and microstructures featuring multiple length scales. While this dataset certainly included sufficient statistical data, the latter complications are notable within the “cloudy zone” region in the data.

Addressing these challenges can be accomplished using a number of different tactics. Longer dwell times can be used to improve the precision of the EDS maps. Higher resolution maps can be performed to address length scale issues and issues with indexing EBSD phase and orientation. In this case, as the meteorite features both extremely large and fine-scale microstructural features, a multi-scale approach is likely the best.

4. CONCLUSION

The application of correlative mechanical microscopy with EDS and EBSD was successfully demonstrated on a fragment of the Seymchan meteorite. All the major features of the investigated area were successfully determined in terms of mechanical properties, orientation, and composition. This was achieved by applying a new open-source python library ‘PyXC’, which can perform correlation on nearly any 2D datasets. By visually comparing correlated maps from the various techniques, the causes of local property variations can often be directly ascertained, such as the correlation between decreases in modulus and increased Ni-concentration. For general trends and phase level properties, correlated statistical datasets clearly illustrate trends between indentation mechanical property clusters and orientation and compositional trends. This demonstrates the potential of this correlative approach for future investigations.

5. ACKNOWLEDGEMENTS

SKK and SHL gratefully acknowledge funding from the European Research Council (ERC) under the European Union’s Horizon 2020 Research and Innovation Programme (Grant Agreement No. 852096 FunBlocks) and the Deutsche Forschungsgemeinschaft (DFG) as part of the Collaborative Research Centre SFB1394 – Structural and Chemical Atomic Complexity – from Defect Phase Diagrams to Material Properties (project ID 409476157 – A05).

6. REFERENCES

- [1] Rossi E, Wheeler J M and Sebastiani M 2023 *Curr. Opinion Solid State Mater. Sci.* **27** 101107
- [2] Seehaus M, Lee S-H, Stollenwerk T, Wheeler J M and Korte-Kerzel S 2023 *Mater. Design* **234** 112296
- [3] Wheeler J M, Gan B and Spolenak R 2022 *Small Methods* **6** 2101084
- [4] Magazzeni C M, Gardner H M, Howe I, Gopon P, Waite J C, Rugg D, Armstrong D E and Wilkinson A J 2021 *J. Mater. Res.* **36** 2235-2250
- [5] Besharatloo H and Wheeler J M 2021 *J. Mater. Res.* **36** 2198-2212
- [6] Oliver W C and Pharr G M 1992 *J. Mater. Res.* **7** 1564-1583
- [7] Phani P S and Oliver W 2019 *Mater. Design* **164** 107563
- [8] Bachmann F, Hielscher R and Schaeben H 2010 *Solid State Phenomena* **160** 63-68
- [9] Wheeler J M 2021 *J. Mater. Res.* **36** 94-104